Cell Death and Survival

Molecular Cancer Research

Autocrine VEGF/VEGFR1 Signaling in a Subpopulation of Cells Associates with Aggressive Osteosarcoma

Tetsuro Ohba[1,7], Justin M.M. Cates[3], Heather A. Cole[1], David A. Slosky[6], Hirotaka Haro[7], Takashi Ando[7], Herbert S. Schwartz[1], and Jonathan G. Schoenecker[1,2,3,4,5]

Abstract

Osteosarcoma is the most common primary bone malignancy and accounts for more than half of primary skeletal malignancies in children and young adults. Although vascular endothelial growth factor (VEGF) expression in osteosarcoma has been associated with poor outcome, its role in the pathogenesis of osteosarcoma remains controversial. Here, VEGF and VEGFR1 expression in both human and murine osteosarcoma cells associated with increasing malignant potential. Autocrine VEGF/VEGFR1 signaling resulted in constitutive activation of VEGFR1 in highly aggressive osteosarcoma cells. In addition, survival and proliferation of highly aggressive osteosarcoma cells was dependent on autocrine VEGF/R1 signaling *in vitro*. The effect of VEGFR1 expression on *in vivo* tumor growth and angiogenesis was evaluated by immunoselecting subpopulations of osteosarcoma cells that express high or low levels of VEGFR1. Cell enriched for high VEGFR1 expression showed increased VEGF production, tumor growth, tumor angiogenesis, and osteolysis *in vivo*. In addition, it was demonstrated that VEGF and VEGFR1 are coexpressed by a subset of tumor cells in human osteosarcoma, similar to what was observed in the murine osteosarcoma cells. These results suggest that autocrine VEGF/VEGFR1 signaling in a subpopulation of tumor cells plays a pivotal role in osteosarcoma progression.

Implications: Aggressive osteosarcoma phenotypes are mediated by autocrine VEGF/VEGFR1 signaling and improved stratification measures and novel anti-angiogenic strategies may benefit this specific tumor type. *Mol Cancer Res; 12(8); 1100–11. ©2014 AACR.*

Introduction

Osteosarcoma is the most common primary bone malignancy in children and young adults and accounts for more than 50% of primary skeletal malignancies in this population. These aggressive tumors commonly metastasize and therefore are routinely treated with neoadjuvant chemotherapy in addition to surgical resection. Despite newly devised poly-chemotherapy regimens combined with wide margin, limb-sparing surgical resection, osteosarcoma continues to confer a poor prognosis in patients who do not respond to chemotherapy or who present with metastatic disease at diagnosis (<30% 5-year survival rate; ref. 1). Consequently, new therapies are needed. Alternative adjuvant therapies designed to inhibit biologic activities, which are crucial for tumor growth and metastasis have increased overall and progression-free survival and decreased morbidity (2, 3). Identifying key molecular mechanisms that drive tumor progression is critical for the development of effective adjuvant therapies.

Vascular endothelial growth factor (VEGF) is overexpressed by the vast majority of solid tumors (4, 5). VEGF includes multiple isoforms. For the purposes of this article, the abbreviation VEGF refers to isoform VEGF-A unless otherwise indicated. Serum VEGF levels are elevated in many patients with cancer, including those with osteosarcoma (6–8). Inhibition of VEGF effectively suppresses osteosarcoma-induced angiogenesis in a murine model of osteosarcoma (9). Unfortunately, the efficacy of anti-VEGF/VEGF receptor (VEGFR) therapy in mouse models have not translated well to clinical efficacy in humans (10), largely because of resistance (11). This generality notwithstanding, regorafenib, a novel oral multi-kinase inhibitor of angiogenic (VEGFR1–3, TIE2), stromal (PDGFRβ, FGFR), and oncogenic kinases (KIT, RET, and RAF) has shown an acceptable safety profile and preliminary evidence of antitumor activity in patients

Authors' Affiliations: Departments of [1]Orthopaedics, [2]Center for Bone Biology, [3]Pathology, Microbiology and Immunology, [4]Pharmacology, [5]Pediatrics, and [6]Cardio-oncology, Vanderbilt University Medical Center, Nashville, Tennessee; and [7]Department of Orthopaedic Surgery, Faculty of Medicine, University of Yamanashi, Chuo, Yamanashi, Japan

Note: Supplementary data for this article are available at Molecular Cancer Research Online (http://mcr.aacrjournals.org/).

Corresponding Author: Jonathan G. Schoenecker, Vanderbilt University Medical Center, 4202 DOT, 2200 Children's Way, Nashville, TN 37232-9565. Phone: 615-936-3080; Fax: 615-343-2423; E-mail: jon.schoenecker@vanderbilt.edu

doi: 10.1158/1541-7786.MCR-14-0037

with solid tumors, including osteosarcoma (12). To understand the molecular pathways responsible for resistance to anti-VEGFR therapy, the mechanisms of osteosarcoma growth and angiogenesis need to be further elucidated.

VEGF receptors [VEGFR1 (flt-1), VEGFR2 (KDR, flk-1), and neuropilin1 (NRP1)] are thought to promote cell proliferation, survival, adhesion, migration, and capillary morphogenesis, VEGFR2 is the primary receptor of VEGF on endothelial cells (13, 14). VEGFR1 has been reported to promote autocrine-stimulated proliferation and cell survival in melanoma and breast carcinoma (15, 16). Here we show that osteosarcoma cells express VEGFR1, but not VEGFR2, and that VEGFR1 expression and activation is associated with increased malignant potential. In addition, only a subpopulation of highly aggressive osteosarcoma cells shows evidence of autocrine signaling through VEGFR1, driving a feed-forward loop upregulating VEGF production and increasing cell proliferation and survival. This cell subpopulation may even drive locoregional angiogenesis within the tumor microenvironment. The results suggest that VEGF/R1 signaling by a relatively small subpopulation of tumor cells may contribute to the aggressive behavior of osteosarcoma.

Materials and Methods

Immortalized osteosarcoma cell lines and culture

Human osteosarcoma lines TE85 and 143B were provided by Dr. H. Luu (Department of Orthopedics, University of Chicago, Chicago, IL; ref. 17). Murine osteosarcoma K-lines initially derived from a primary osteosarcoma in a Balb/C mouse (18) were provided by Dr. E. Kleinerman (Department of Pediatrics, University of Texas M.D. Anderson Cancer Center, Houston, TX) and bEnd.3 mouse endothelioma cells (19) were obtained from the American Type Culture Collection. All cells were maintained in complete Dulbecco's Modified Eagle Medium (DMEM; Invitrogen Life Technologies) supplemented with 10% fetal calf serum (FBS; HyClone/Thermoscientific) with 5.0% antimycotic solution (Invitrogen Life Technologies) at 37°C in a humidified normoxic atmosphere in the presence of 5% CO_2.

Measures of cell viability, proliferation, and apoptosis

Viability. For methyl-tetrazolium bromide mitochondrial activity assay (MTT), human or murine cells were plated in 96-well plates (7.0×10^3 cells/well), and incubated for 4 hours in 100 μL growth media, after which cells were cultured in serum-free medium for an additional 24 hours. Cells were then exposed to indicated doses of mouse $VEGF_{164}$ (R&D Systems Inc.), human $VEGF_{165}$ (R&D Systems Inc.), VEGF-E (Abcam), TGFβRI Kinase Inhibitor (HTS 466284), VEGFR1 kinase inhibitor (NITVLKKFPL, EMD Millipore), or anti-mouse $VEGF_{164}$ antibody (R&D Systems Inc.) in serum-free media for 24 hours. Subsequently, 20 μL of MTT reagent (CellTiter 96 AQueous 1 Solution Reagent; Promega) was added for 4 hours. Absorbance was measured at 490 nm with a microplate reader (Biotek).

Proliferation. Bromodeoxyuridine (BrdUrd) incorporation assays were performed as recommended by the manufacturer (Cell Proliferation ELISA, BrdU Kit; Roche). K7M3 and K12 cells were incubated in serum-free media for 18 hours as described for the MTT assay. Absorbance was measured at 370 nm.

Measures of cell apoptosis. Human or murine cells (8×10^5 cells/well) were plated on 6-well plates and incubated for 6 hours in 100 μL growth media. Cells were exposed to 40 μmol/L TGFβRI kinase inhibitor or VEGFR1 kinase inhibitor for 24 hours and then trypsinized and pelleted by centrifugation. Cell pellets were washed with PBS twice and resuspended in 300 μL binding buffer at a density of 1×10^6 cells/mL. To detect apoptosis, 100 μL of the cell suspension was analyzed by flow cytometry (BD FACSCantoII) after cells were stained with 1 μL Annexin V-FITC and 10 μL propidium iodide solution (Trevigen Inc.).

Transcription of small interfering RNA. K7M3 cells were cultured (5×10^5 cells/well) for 24 hours in 6-well plates in DMEM with 10% FBS and were transiently transfected with 10 or 50 pmol/L siVEGFR1 (Mm.389712) or siControl (#4390843) using the Silencer Select small interfering RNA (siRNA) system (Invitrogen Life Technologies). For transfections, Lipofectamine 2000 reagent (Invitrogen) was used according to the manufacturer's instructions.

RT-PCR amplification. Total RNA was isolated from murine cell lines using RNeasy (Qiagen). Aliquots of 1 μg of total RNA were converted to cDNA by RT synthesized with SuperScript-III reverse transcriptase (Invitrogen Life Technologies) using oligo-dT primers (Sigma-Aldrich). Subsequently, polymerase chain reaction (PCR) was performed using Taq polymerase (Qiagen) in a total reaction volume of 25 μL. The oligonucleotide sequences of the primers were as follows:

Mouse VEGFR1	Forward, CGCTTTTTGTCAGTCATCTTCA
	Reverse, TCTCGGCATTCACTTTGGTC
Mouse VEGFA	Forward, CGGGTGCAGGCATTCCAGAG
	Reverse, CTCCGTGGGACAGAGAGGAC
Mouse VEGFR2	Forward, TACACAATTCAGAGCGATGTGTGGT
	Reverse, CTGGTTCCTCCAATGGGATATCTTC
Mouse β-actin	Forward, TGGAATCCTGTGGCATC
	Reverse, TAAAACGCAGCTCAGTAACAGTCCG

Cycling conditions were 92°C for 2.5 minutes, 59°C for 1 minute, and 72°C for 1 minute, followed by one extension cycle at 72°C for 5 minutes. VEGFR1 and VEGFR2 was amplified over 35 cycles, VEGF-A over 33 cycles, and β-actin over 22 cycles. PCR was performed in a DNA Thermal Cycler (Biometra). The amplified DNA was then electrophoresed on a 2% agarose gel and visualized by SYBR Safe DNA Gel Stain (Invitrogen Life Technologies).

Quantitative real-time PCR. Total RNA was isolated from murine cell lines using RNeasy (Qiagen) and cDNA

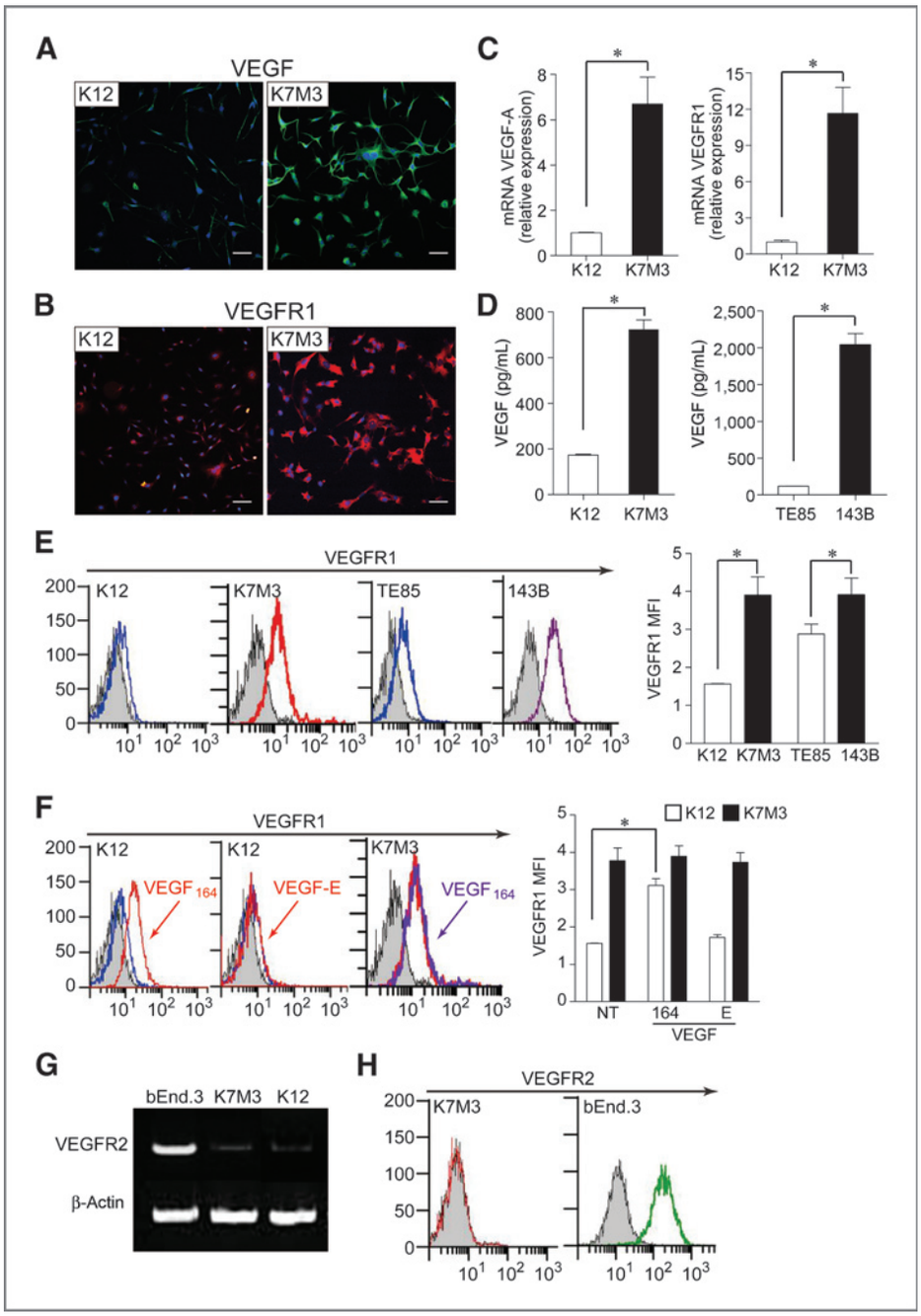

Figure 1. VEGF and VEGFR1 expression in murine osteosarcoma cell lines are associated with increased malignant potential. A and B, immunofluorescence staining of K12 or K7M3 osteosarcoma cells for VEGF (green) and VEGFR1 (red). Scale bar, 100 μm. C, VEGF-A and VEGFR1 mRNA expression was quantified in unsorted and immunosorted K7M3 cells by quantitative RT-PCR using primers for VEGF-A, VEGFR1, and GAPDH. The ratios of VEGF-A and VEGFR1 mRNA levels were normalized to those of GAPDH. Values are means of relative expression levels ± SD from 2 independent experiments (*, $P < 0.01$ compared with untreated control). D, K12 and K7M3 cells were cultured for 48 hours and VEGF levels were measured in conditioned media by ELISA. Values, mean ± SD of 3 independent experiments (*, $P < 0.01$). E, surface VEGFR1 expression on osteosarcoma cell lines was assessed by flow cytometry and displayed graphically in right (gray plots, IgG-isotype controls). Values plotted are median fluorescent intensity (MFI) ± SD from 3 independent experiments (*, $P < 0.01$). F, K12 or K7M3 cells were cultured in the presence or absence of 100 ng/mL of $VEGF_{164}$ or VEGF-E for 24 hours and subsequently analyzed for surface VEGFR1 by flow cytometry. For K12 cells, the blue plot indicates untreated cells and red plot indicates VEGF-stimulated cells (gray plots indicate IgG-isotype controls). For K7M3 cells, the red plot indicates untreated cells and the purple plot indicates VEGF-stimulated cells. Data are representative of 3 independent experiments summarized in the graphic in right. Values plotted are median fluorescent intensity (MFI) ± SD (*, $P < 0.01$). G, VEGFR2 mRNA expression in bEnd.3 cells, K7M3, K12 cells was assessed by RT-PCR. Data shown are representative of 2 independent experiments. H, surface VEGFR2 expression on osteosarcoma cell lines was assessed by flow cytometry. bEnd.3 mouse endothelial cells were used as positive control (gray plots indicated IgG-isotype control).

was then synthesized using the High-Capacity cDNA Reverse Transcription Kit (Applied Biosystems). Quantitative RT-PCR analysis of individual cDNA was performed with ABI Prism 7500 (Applied Biosystems) using TaqMan Gene Expression Assays (Applied Biosystems; VEGFA, Mm00437304_m1; VEGFR1, Mm00438980_m1, GAPDH, Mm99999915_g1). mRNA expression levels were normalized to the mean expression of GAPDH.

Flow cytometry. Murine osteosarcoma K-lines were cultured in 6-well plates for 24 hours in DMEM with 10% FBS, and then exposed to recombinant mouse $VEGF_{164}$ or VEGF-E for 24 hours in serum-free media. For measurement of surface VEGFR1 and VEGFR2 expression, human or murine cells were retrieved using Cell Stripper (Cellgro) and incubated with anti-human or murine VEGFR1, VEGFR2, or isotype control (normal goat IgG; AB-108-C; R&D Systems Inc.) for 30 minutes. Human or murine cells were then incubated with secondary antibody (Alexa Fluor 647; Molecular Probes, Invitrogen). Data were collected using a FACSCantoII (BDBiosciences) and analyzed with WinList software (Verity Software House). Light scatter was gated to exclude debris, dead cells, and aggregates, and Alexa Fluor 647 fluorescence intensity compared.

Cell isolation. Subsets of murine K7M3 cells were stained as above for isolation of the highest (95% cutoff) and lowest (5% cutoff) levels of VEGFR1 expression by fluorescence-activated cell sorting on a FACSAriaII (BDBiosciences).

Cellular immunofluorescence. Murine cells were fixed 3.7% formaldehyde in PBS for 10 minutes with (for VEGF) or without (for VEGFR1) permeabilization using 0.1% TritonX-100 (Fisher Scientific). After blocking in 5% normal goat serum/0.1% Triton/PBS, cells were incubated with anti-VEGFR1 antibody or normal rabbit control IgG (Abcam) overnight at 4°C. Sections were then incubated in Alexa Fluor 594–conjugated secondary antibody (Molecular Probes, Invitrogen). Images were collected using an NIKON AZ100 microscope.

Enzyme-linked immunosorbent assay. Human or murine cell lines were grown in 6-well plates. At approximately 75% confluence, cells were washed with PBS and fresh serum-free medium was added. After 48 hours, conditioned medium was collected and cells were counted with a hemocytometer (Fisher Scientific). CM was then tested with Quantikine quantitative colorimetric enzyme-linked immunosorbent assay (ELISA) for human or murine VEGF according to the manufacturer's specifications (R&D Systems Inc.). For plasma analysis, mouse blood was collected in tubes containing 0.109 M sodium citrate. Platelet-free plasma was prepared by double microcentrifugation at $1,500 \times g$ for 15 minutes followed by centrifugation of supernatant at $13,000 \times g$ for 15 minutes. Concentrations of VEGF (R&D Systems Inc.) in mouse plasma were determined by ELISA.

VEGFR1 phosphorylation assay. Murine cells were plated in 96-well plates (2.5×10^4 cells/well) and incubated for 4 hours in 100 μL growth media. After culture in serum-free medium for an additional 4 hours, cells were exposed to $VEGF_{164}$, anti-$VEGF_{164}$ antibody, or VEGFR1 kinase inhibitor in serum-free media for 10 to 30 minutes at 37°C. Subsequently, 100 μL of 4% paraformaldehyde solution was added for 20 minutes. After 1 hour treatment with blocking solution (Ray Biotech) at 37°C, cells were incubated with anti-phospho-VEGFR1 (Y1333) antibody (Abcam) for 2 hours followed by anti-rabbit IgG, HRP-linked antibody (Ray Biotech), and TMB One-Step Substrate Reagent (Ray Biotech) for 30 minutes at room temperature. Absorbance was measured at 450 nm with a microplate reader (Biotek).

Cell migration assay. The cell migration assay was performed using a modified Boyden transwell chamber (8-mm pore size). K7M3 cells were added to the upper chamber with or without 20 μmol/L VEGFR1 kinase inhibitor or 0.1 μg/mL antimouse VEGF antibody (R&D Systems Inc.). Basal migration and K7M3 cell–directed migration were determined after 24 hours. Nonmigrating cells on the upper surface of the filter were wiped off with a cotton swab and migrating cells adherent to the lower surface were fixed with 10% formaldehyde. Cells that had migrated to the lower surface were quantified by colorimetric measurement following staining with 1% crystal violet. Absorbance was measured at 590 nm with a microplate reader (Biotek).

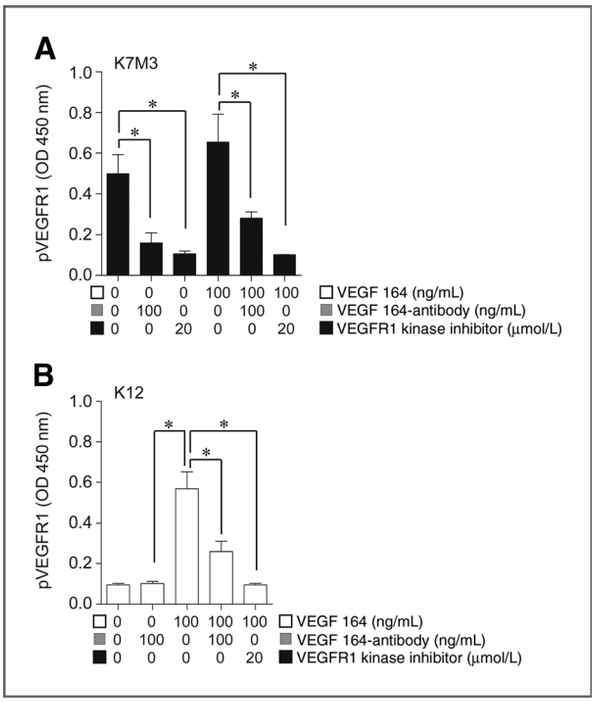

Figure 2. Autocrine VEGF/R1 signaling in aggressive K7M3 osteosarcoma cells, but not in less aggressive K12 cells. A and B, K7M3 or K12 cells were cultured in the presence or absence of 100 ng/mL of $VEGF_{164}$ with or without 100 ng/mL anti-$VEGF_{164}$ antibody or 20 μmol/L VEGFR1 kinase inhibitor for 20 minutes and subsequently analyzed for VEGFR1 phosphorylation by cell-based ELISA. Absorbance was quantified at 450 nm (OD 450). Data represent the mean ± SD from 2 independent experiments (*, $P < 0.01$).

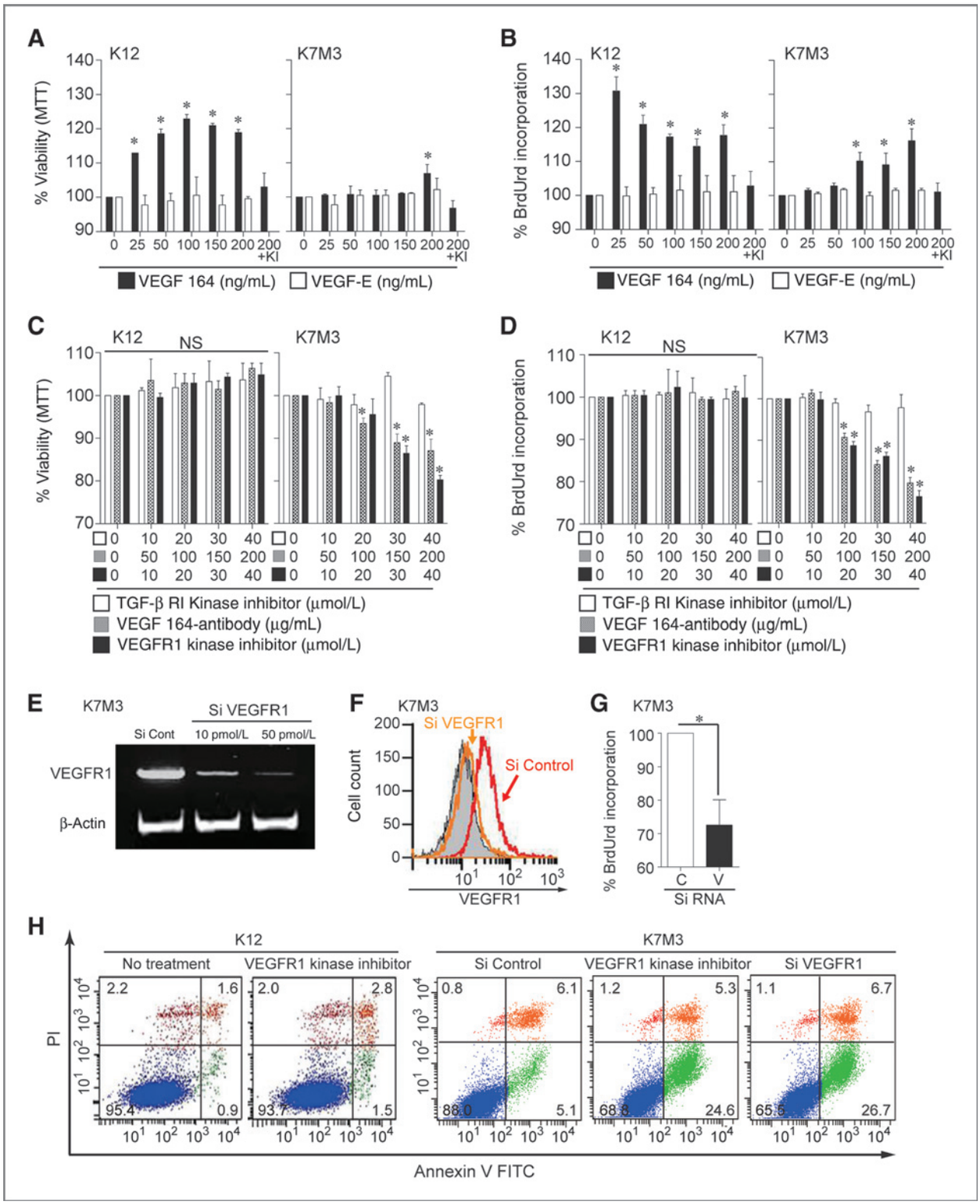

Figure 3. Autocrine VEGF/R1 signaling stimulates cell proliferation and inhibits apoptosis in aggressive K7M3 osteosarcoma cells, but not in less aggressive K12 cells. A and B, viability and proliferation of K12 and K7M3 cells were measured by MTT (A) and BrdUrd (B) incorporation assays at baseline and in the presence of increasing concentrations of $VEGF_{164}$ or VEGF-E with or without 20 μmol/L VEGFR1 kinase inhibitor over 24 hours. Values are means ± SD of the percentage increase compared with baseline from 3 independent experiments (* $P < 0.01$ compared with corresponding control). (*Continued on the following page.*)

In vivo osteosarcoma model

Animals. All animal care was approved by the Vanderbilt Medical Center Institutional Animal Care and Use Committee. Balb/C mice (Jackson Laboratories) were housed at 22°C to 24°C with a 12-hour light/dark cycle with standard mouse chow and water provided *ad libitum*. Single-cell suspensions (1×10^5) of K12, K7M3, or K7M3 cells sorted by VEGFR1 expression level were injected into the right tibias of 15 6-week-old male mice (VEGFR1-low cells, $n = 7$; VEGFR1-high cells, $n = 8$) as previously described (20). Mice were sacrificed after 4 weeks (10 weeks of age) by CO_2 inhalation.

Analysis of tumor growth. Mice were observed daily for signs of tumor growth, including limping. Weekly radiographic evaluations were performed using a LX-60 Radiography System (Faxitron X Ray; 8 seconds at 35 kV). Assessment of the soft tissue silhouette surrounding the injected tibia was conducted by analysis of radiographs using Image J (version 1.44 u; NIH) as previously described (21). Tumor growth was calculated weekly as the percentage increase in size of the injected tibia compared with the paired contralateral control.

Histologic analysis. Long bones were fixed in 4% paraformaldehyde and then decalcified with 10% EDTA. Bones were then paraffin-embedded and consecutive 7 μm sections were stained with hematoxylin and eosin (H&E). Immunofluorescence for VEGF, VEGFR1, or Ki67 (Abcam) was performed using Alexa Fluor 647 (A212244; Life Technologies) and DAPI counterstain (D3571; Invitrogen) according to the manufacturer's protocol and imaged with Nikon AZ100M fluorescent microscope (Nikon). Images were captured and analyzed with MetaMorph image analysis software (Molecular Devices).

Angiographic method with barium sulfate technique. Mice were anesthetized and laid supine to gain access to the thoracic and abdominal cavities. A midline incision was made and the heart was exposed through a midline sternotomy. The left ventricle was accessed using a 25 G butterfly needle. The suprahepatic inferior vena cava (IVC) was transected for drainage and the vasculature was subsequently perfused with 9 mL of warm heparinized saline (100 U/mL in 0.9% saline). Complete exsanguination was documented by complete blanching of the liver and obtaining clear fluid from the IVC. Vascular contrast polymer was prepared by mixing 10 g of VARIBAR (E-Z-EM) with 10 mL of 10% (v/v) gelatin (Sigma-Aldrich) and progressively infused manually into the left ventricle. Adequate filling of the arterial system was documented by distension of the visceral and body cavity vasculature by white silicone rubber solution. Previous studies have found that this observation corresponds to a physiologic pressure of 100 to 120 mm Hg (22). Mice were stored at 4°C overnight to allow the vascular contrast to polymerize, and then fixed in 4% PFA for 72 hours. Both femurs were then carefully macrodissected and analyzed by radiography and micro-computed tomography (μCT) before and after demineralization with 10% (v/v) HCl.

Micro-computed tomography. Barium sulfate vascular contrast was imaged using an X-ray computed tomography scanner (μCT40; Scanco Medical) at 55 kVp/145 μA with an integration time of 200 milliseconds and 1,000 projections per 360° rotation giving 20-μm voxels (isotropic). Vascular contrast area (% area) was quantified using Metamorph software (Molecular Devices). In addition, extent of osteolysis was determined by microcomputed X-ray tomography (μCT40; Scanco Medical AG) of the trabecular bone volume within the tibial metaphysis via contiguous cross sections of the metaphyseal region (70 kV, 114 lA, 300 milliseconds integration, 500 projections per 180° rotations, with a 12 μm isotropic voxel size).

Statistics

One-way analysis of variance (ANOVA) with Bonferroni multiple 2-sided comparison tests and posttest for trend were used to analyze *in vitro* and *in vivo* animal model experiments. Correlations between tumor size and plasma markers were determined by Pearson's correlation coefficient. All statistical calculations were determined using Prism v4.0 (Graph Pad Software). For all tests, $P < 0.05$ was considered statistically significant.

Results

VEGF and VEGFR1 expression in human and murine osteosarcoma cell lines is associated with increased malignant potential

The associations between VEGF and VEGFR1 expression and the malignant phenotype of osteosarcoma cell lines *in vitro* were examined. The malignant potential or biologic aggressiveness of the cell lines utilized were defined by their rate of orthotopic primary tumor growth and spontaneous

(*Continued*.) KI denotes VEGFR1 kinase inhibitor. C and D, viability and proliferation of K12 and K7M3 cells were measured by MTT (C) and BrdUrd incorporation assays (D) at baseline and in the presence of increasing concentrations of anti-$VEGF_{164}$ antibody, VEGFR1 kinase inhibitor, or a TGFβR1 kinase inhibitor over 24 hours. Values are means ± SD of the percentage increase compared with baseline from 3 independent experiments (*, $P < 0.01$ compared with corresponding control, NS, $P > 0.05$). E, K7M3 cells were treated with 10 or 50 pmol/L siRNA-control or siRNA-VEGFR1 for 24 hours before RNA extraction and VEGFR1 expression was assessed by RT-PCR. Data shown are representative of 2 independent experiments. F, surface VEGFR1 expression on K7M3 cells treated with 50 pmol/L siRNA-control or siRNA-RANKL for 72 hours was analyzed using flow cytometry. Data are representative of 2 independent experiments. G, proliferation of K7M3 cells treated with 50 pmol/L siRNA-control (C) or siRNA-VEGFR1 (V) for 72 hours were measured by BrdUrd incorporation assays. Values are means ± SD of the percentage increase compared with baseline from 2 independent experiments (*, $P < 0.01$). H, apoptosis of K12 and K7M3 cells was assessed by flow cytometry. K12 or K7M3 cells were treated with 30 μmol/L VEGFR1 kinase inhibitor for 24 hours and then stained with Annexin V-FITC/PI for flow cytometry. Apoptosis of K7M3 cells treated with 50 pmol/L siRNA-control or siRNA-VEGFR1 for 72 hours was also assessed by flow cytometry. The percentage of Annexin V-positive, low-PI staining cells (early apoptosis, green dots) in treated cells were compared with untreated cells or siRNA control–treated cells. Representative data from 3 independent experiments are shown. Healthy cells are represented in the lower left quadrant (blue), early apoptotic cells in the lower right quadrant (green), late apoptotic cells in the upper right quadrant (orange), and necrotic cells in the upper left quadrant (red).

pulmonary metastases. The clonally related murine osteosarcoma K-cell lines show a highly aggressive (K7M3) and less aggressive (K12) model phenotype (23, 24). Similarly, the human 143B cell line is much more aggressive than the respective parental cell line (TE85), with greater tumorigenic and metastatic potential (17).

Immunofluorescence microscopy demonstrated increased intensity of VEGF and VEGFR1 in aggressive K7M3 cells compared with parental K12 cells (Fig. 1A and B). Both VEGF and VEGFR1 mRNA levels determined by qRT-PCR were higher in K7M3 cells than in K12 cells (Fig. 1C). Likewise, VEGF levels detected in CM from aggressive osteosarcoma cells (K7M3 and 143B) were significantly greater than those in CM from K12 and TE85 cells (Fig. 1D). Flow cytometry also showed that VEGFR1 expression is significantly higher in aggressive

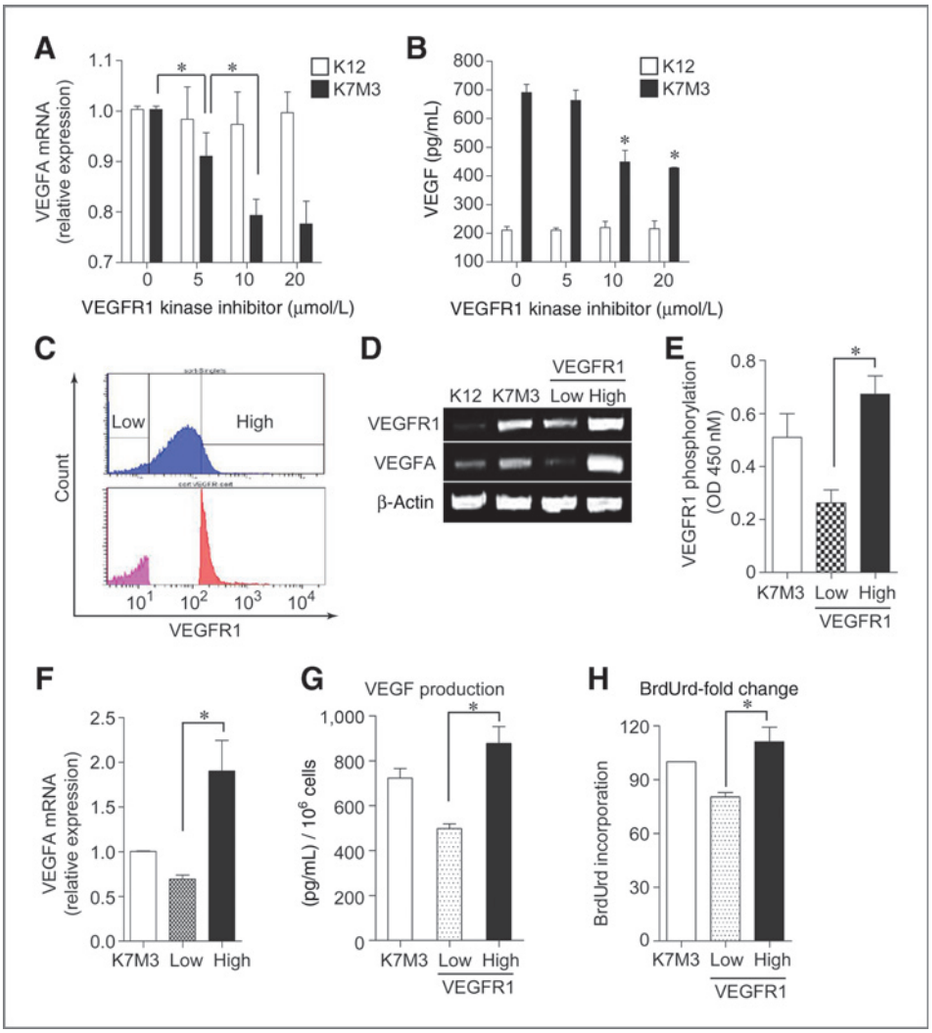

Figure 4. Autocrine VEGF/R1 signaling stimulates VEGF-A expression in aggressive K7M3 cells, but not in K12 cells. A, K12 or K7M3 cells were cultured with increasing concentrations of VEGFR1 kinase inhibitor for 12 hours before RNA extraction and quantitative RT-PCR using primers for VEGF-A and GAPDH. The ratio of VEGF-A mRNA levels was normalized to that of GAPDH. Values are means of relative expression levels ± SD from 3 independent experiments (*, $P <$ 0.01 compared with untreated control). B, K12 or K7M3 cells were cultured with increasing concentrations of VEGFR1 kinase inhibitor for 48 hours and CM was collected for determination of VEGF concentration by ELISA. Values presented are means ± SD from 3 independent experiments (*, $P < 0.01$ compared with untreated cells). C, K7M3 cells were preincubated with anti-VEGFR1 antibody and immunosorted by flow cytometry. High VEGFR1-expressing cells (≥95th percentile) and low VEGFR1-expressing cells (≤5th percentile) were immunoselected for further study (bottom). D, VEGF-A and VEGFR1 mRNA expression in immunosorted K7M3 cells, unsorted K7M3 cells, and K12 cells was assessed by RT-PCR. Data shown are representative of 2 independent experiments. E, VEGFR1-high–expressing K7M3 cells or VEGFR1-low–expressing K7M3 cells were cultured and subsequently analyzed for VEGFR1 phosphorylation by cell-based ELISA. Values presented are means ± SD from 2 independent experiments (*, $P < 0.01$). F, VEGF-A mRNA expression was quantified in unsorted and immunosorted K7M3 cells by quantitative RT-PCR using primers for VEGF-A and GAPDH. The ratio of VEGF-A mRNA levels was normalized to that of GAPDH. Values are means of relative expression levels ± SD from 2 independent experiments (*, $P < 0.01$ compared with untreated control). G, VEGF-A production by unsorted and immunosorted K7M3 cells was assessed by ELISA of conditioned media after 48 hours. Values presented are means ± SD from 3 independent experiments (*, $P < 0.01$). H, proliferative capacity of unsorted and immunosorted K7M3 cells was assessed by BrdUrd incorporation. Values are the mean fold change ± SD from 2 independent experiments (*, $P < 0.01$).

143B and K7M3 osteosarcoma cells compared with parental TE85 and K12 cells, respectively (Fig. 1E). Thus, both VEGF and VEGFR1 expression correlate with the inherent malignant potential of human and murine osteosarcoma cell lines. VEGFR1 expression by K12 cells was significantly increased by exogenous $VEGF_{164}$ (one of many splice variants of the mouse VEGF-A gene), but not VEGF-E [which cannot bind to VEGFR1 (13); Fig. 1F]. In contrast, VEGFR1 expression by K7M3 was not increased over baseline levels by $VEGF_{164}$ treatment (Fig. 1F). VEGFR2 was not detectable in these osteosarcoma cell lines by RT-PCR or flow cytometry (Fig. 1G and H).

Autocrine signaling results in constitutive activation of VEGFR1 in highly aggressive osteosarcoma cells

Phosphorylated VEGFR1 is present at high levels in K7M3 cells, but not K12 cells (Fig. 2A and B). Both anti-$VEGF_{164}$ antibody and VEGFR1 kinase inhibitor significantly decrease VEGFR1 phosphorylation in K7M3 cells, but not K12 cells. Although exogenous $VEGF_{164}$ strongly induced VEGFR1 phosphorylation in K12 cells, it only had a slight effect on K7M3 cells (Fig. 2A and B). These results suggest that autocrine VEGF/R1 signaling results in constitutive activation on VEGFR1 in the highly aggressive osteosarcoma cell line K7M3, but not in the less aggressive K12 cells.

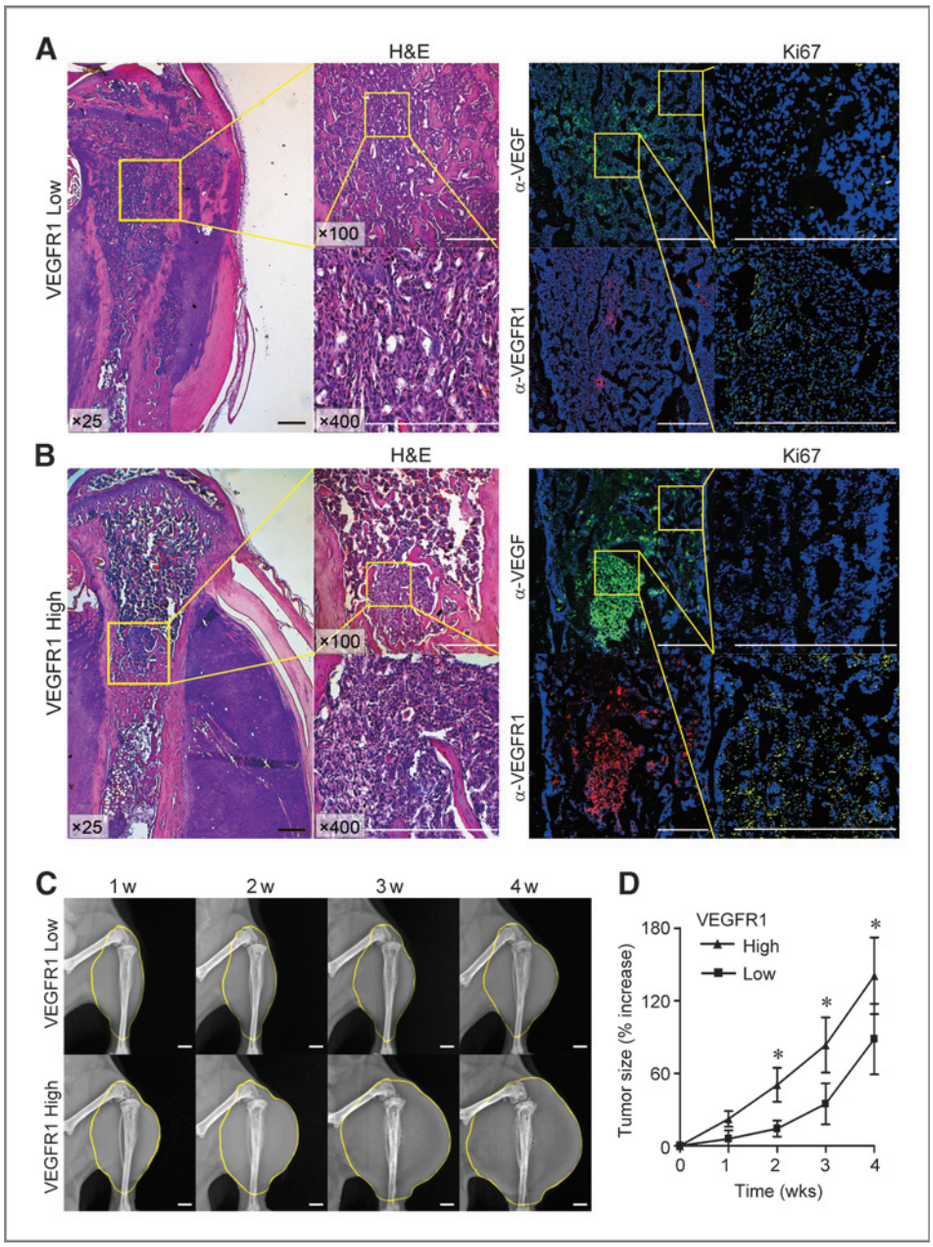

Figure 5. VEGFR1-high–expressing K7M3 cells are more aggressive than VEGFR1-low–expressing K7M3 cells *in vivo*. A and B, single-cell suspensions (1×10^5) of K7M3 cells immunsorted for VEGFR1 expression level were injected into tibias. Immunolocalization of VEGF-A, VEGFR1, and Ki67-positive cells was performed 4 weeks after injection with VEGFR1-low expressing (A, $n = 7$) or VEGFR1-high–expressing (B, $n = 8$) K7M3 cells (magnification ×25 or ×100 or ×400; scale bar, 500 μm). Immunolocalization of Ki67 is demonstrated for representative areas with increased or negligible VEGF-A immunoreactivity. C, tumor growth was quantified by measuring the soft-tissue silhouettes in serial radiographs to determine the percentage increase in area compared with the contralateral noninjected control tibia (scale bar, 1 mm). D, plots of *in vivo* tumor growth of VEGFR1-high–expressing K7M3 cells ($n = 8$) compared with VEGFR1-low–expressing K7M3 cells ($n = 7$; *, $P < 0.01$ compared with paired time point).

Proliferation and cell survival of highly malignant osteosarcoma cells is dependent on VEGF/R1 autocrine signaling *in vitro*

Exogenous VEGF-A, but not VEGF-E, stimulated cellular proliferation and viability in the less aggressive osteosarcoma cell lines (K12) as measured by MTT assays and BrdUrd assays (Fig. 3A and B). In contrast, VEGF-A had negligible effects on the aggressive osteosarcoma cell lines (K7M3) at levels <100 ng/mL (Fig. 3A and B). In addition, the VEGFR1 kinase inhibitor diminished the effect of $VEGF_{164}$ proliferation and viability of both K12 and K7M3 cells (Fig. 3A and B).

Inhibition of VEGF/R1 signaling by anti-$VEGF_{164}$ antibody or VEGFR1 kinase inhibitor significantly decreased cell viability and cell proliferation of K7M3 cells, while blocking TGFβ signaling with a TGFβR1 kinase inhibitor had no effect (Fig. 3C and D). In contrast, inhibition of VEGF/R1 signaling does not affect the parental K12 cells. The effect of VEGF/R1 signaling on apoptosis of human and murine osteosarcoma cells was also assessed by flow cytometry (Fig. 3H and Supplementary Fig. S1C). The percentage of apoptotic K7M3 cells increased 5-fold upon treatment with 30 μmol/L VEGFR1 kinase inhibitor, but there was no significant increase in apoptosis of K12 cells (Fig. 3E).

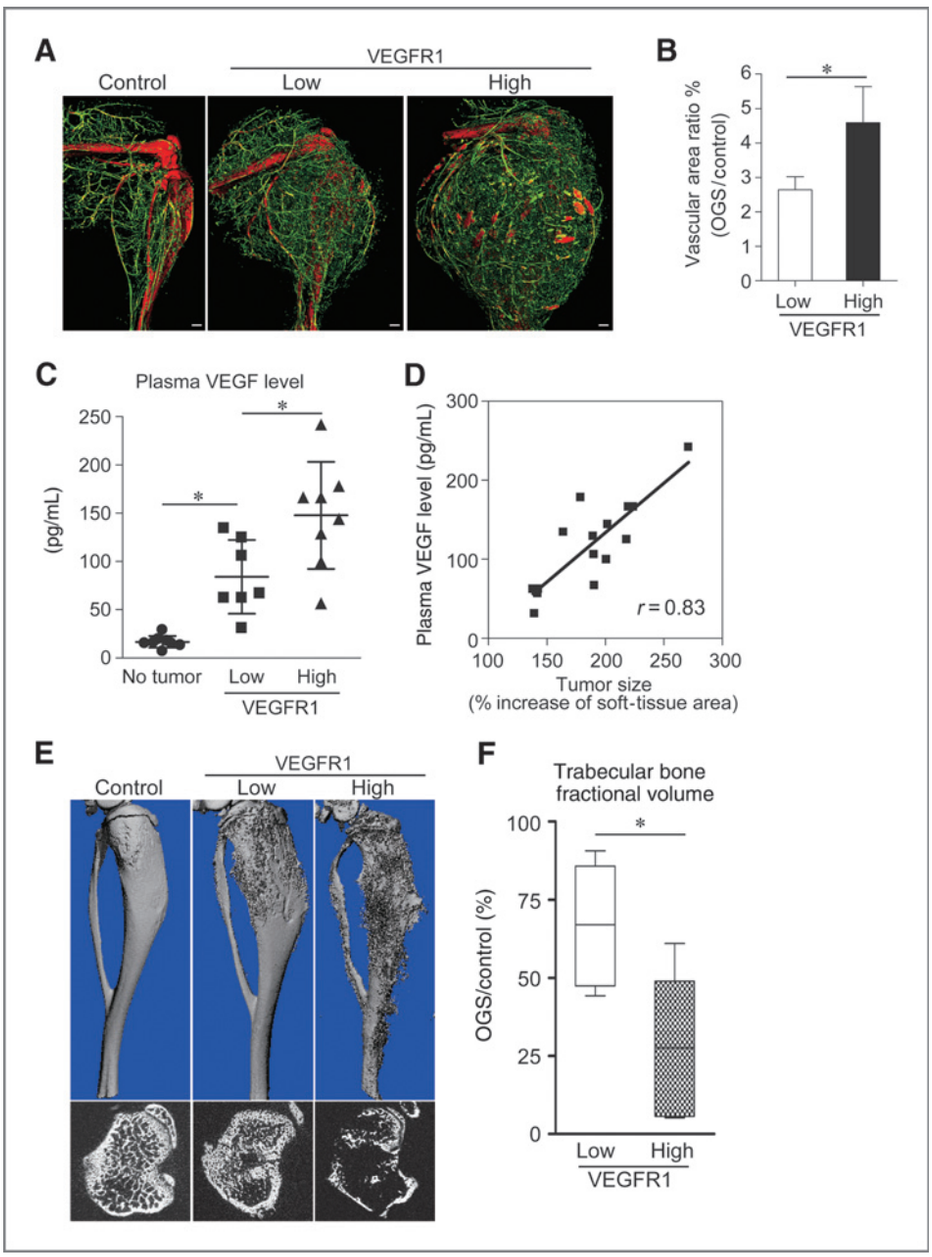

Figure 6. VEGFR1-high–expressing K7M3 cells are associated with increased tumor vascularity and tumor-induced osteolysis *in vivo*. A, representative images of 3-dimensional reconstructions of angiography studies demonstrate the amount of osteosarcoma-associated vasculature 4 weeks after tumor cell inoculation. Scale bar, 1 mm. B, quantification of tumor bed vascular volume normalized to contralateral tumor-free tibia. Data are from 3 animals per group (*, $P < 0.01$). C, plasma VEGF levels from control (no tumor) mice or tumor-bearing mice injected with VEGFR1-high or VEGFR1-low K7M3 cells were measured by ELISA. (Control, $n = 8$; VEGFR1-low, $n = 7$; VEGFR1-high, $n = 8$; *, $P < 0.01$). D, plasma VEGF levels positively correlated with tumor burden assessed by radiographic analysis ($n = 15$, $P = 0.0001$). E, tumor-bearing tibias injected with VEGFR1-high or VEGFR1-low expressing K7M3 cells were compared with noninjected control tibias by μCT 4 weeks after tumor cell inoculation (top, 3D reconstructions; bottom, transverse images; scale bar, 1 mm). F, bone fractional volume measurements at metaphyses of tibias injected with VEGFR1-high and VEGFR1-low–expressing K7M3 cells was determined by μCT and normalized to the contralateral control tibial metaphysis. Representative images from animals injected with VEGFR1-high cells ($n = 5$) and VEGFR1-low cells ($n = 4$) are shown. Values, mean ± SD (*, $P < 0.01$).

Similar findings were observed in human aggressive osteosarcoma 143B cells and parental TE85 cells (Supplementary Fig. S1A–S1C).

To clarify the importance of VEGFR1 expression in K7M3 cells, we demonstrated that siRNA-mediated knockdown of VEGFR1 expression in K7M3 cells significantly decreased cell proliferation and induced apoptosis of K7M3 cells (Fig. 1E–H). Together, these results indicate that whereas the nonaggressive cell line (K12) can be stimulated by VEGF to promote proliferation and cell viability, the aggressive K7M3 cell line is insensitive to additional exogenous VEGF, presumably because of endogenous activation of VEGFR1 signaling. In addition, VEGF/R inhibition decreased the migratory potential of K7M3 cells (Supplementary Fig. S2A and S2B).

VEGFR1 signaling stimulates VEGFA production in aggressive K7M3 cells

To investigate the effect of inhibiting VEGFR1 on VEGF secretion by osteosarcoma K-lines *in vitro*, we treated K12 or K7M3 cells with increasing concentrations of VEGFR1 kinase inhibitor and assessed VEGF-A mRNA and protein levels. Upon kinase inhibition, VEGF-A mRNA levels were decreased in K7M3 cells, but not in K12 cells (Fig. 4A). These findings were corroborated by ELISA of VEGF in CM from VEGFR1-inhibited K-cells (Fig. 4B). The effects of VEGFR1 inhibition on VEGF expression in K7M3 cells were concentration dependent in both assays. These results indicate that VEGF expression in K7M3 cells, but not K12 cells, is stimulated by VEGFR1 signaling.

Based on these findings, we hypothesized that autocrine VEGF/R1 signaling may be a determinant of aggressive potential in osteosarcoma. Subpopulations of K7M3 cells that express the highest ($\geq$95th percentile) and lowest ($\leq$5th percentile) levels of VEGFR1 were isolated by cell sorting using immuno-magnetic selection (Fig. 4C). VEGFR1 mRNA levels determined by RT-PCR were higher in the VEGFR1-high K7M3 cells compared with VEGFR1-low K7M3 cells and K12 cells (Fig. 4D). Phosphorylated VEGFR1 was also higher in VEGFR1-high K7M3 cells compared with VEGFR1-low K7M3 cells (Fig. 4E). Similar findings were observed when VEGF expression was measured by qRT-PCR or ELISA of CM from the different cell K7M3 populations (Fig. 4F and G). High VEGFR1 activity was associated with increased VEGF levels, suggesting that VEGF expression is driven by VEGFR1 and that an autocrine feedback loop is active in a subset of K7M3 cells. Importantly, VEGFR1-high K7M3 cells also showed significantly greater proliferative potential than VEGFR1-low K7M3 cells (Fig. 4H). These results suggest that VEGF/R1 autocrine signaling is associated with an aggressive phenotype of K7M3 cells.

High VEGFR1 expression is associated with increased tumor growth and angiogenesis *in vivo*

To evaluate effects of high or low VEGFR1 expression on osteosarcoma growth *in vivo*, we injected the separate K7M3 subpopulations selected by VEGFR1 expression level into mouse tibias. VEGFR1-high K7M3 cells formed significantly larger tumors than VEGFR1-low K7M3 cells as determined by serial radiographs (Fig. 5A and B). Consistent with our *in vitro* data, tumors formed by VEGFR1-high K7M3 cells show more intense immunolabeling for VEGF and VEGFR1 than tumors formed by VEGFR1-low K7M3 cells (Fig. 5C and D). In addition, immunofluorescence for Ki67 showed a higher proliferative index in VEGFR1-high tumors. The proliferative regions in osteosarcoma colocalized to areas of high VEGF and VEGFR1 expression (Fig. 5C and D).

Angiography with a barium sulfate emulsion was used to demonstrate neoangiogenesis in osteosarcoma. VEGFR1-high K7M3 cells showed a larger vascular bed compared with that induced by VEGFR1-low K7M3 cells (Fig. 6A and B). Plasma levels of VEGF were also significantly higher in animals injected with VEGFR1-high K7M3 cells compared with VEGFR1-low K7M3 cells (Fig. 6C). Plasma VEGF levels strongly correlated with tumor size (Fig. 6D). In addition, μCT analysis at 4 weeks postinjection showed that VEGFR1-high K7M3 cells caused significantly more tumor-associated osteolysis compared with that induced by VEGFR1-low K7M3 cells (Fig. 6E and F).

Colocalization of VEGF/VEGFR1 in human osteosarcoma

To investigate the clinical relevance of our findings, immunofluorescence microscopy for anti-VEGFR1 and anti-VEGF was performed on chemotherapy-naïve (n = 2) and adjuvantly treated (n = 8) human osteosarcoma samples. VEGF and VEGFR1 were found to be co-expressed only on a subset of tumor cells in human osteosarcoma (Fig. 7A–D and Supplementary Fig. S3). That VEGF and VEGFR1 are coexpressed on a subset of osteosarcoma cells

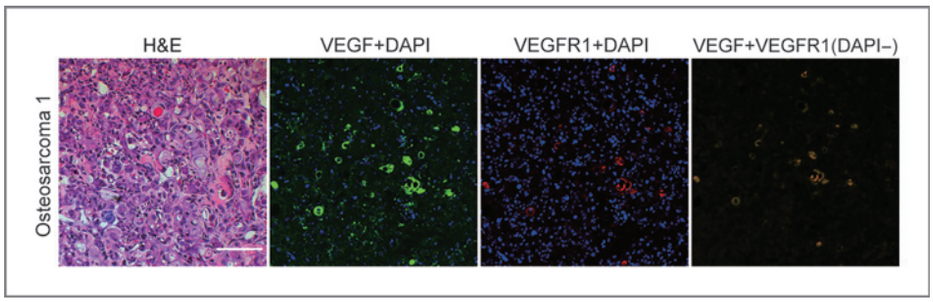

Figure 7. Representative chemotherapy-naïve human osteosarcoma tissue was stained by immunofluorescence for VEGF (green) or VEGFR1 (red). Merged images (yellow) demonstrate coexpression of VEGFR and VEGFR1 in a subpopulation of human osteosarcoma cells (magnification ×200; scale bar, 100 μm).

further suggests that these tumors are composed of a heterogeneous population of cells, some of which seem to activate VEGF/R1 signaling in autocrine fashion.

Discussion

It is crucial to understand the molecular mechanisms responsible for clinically aggressive behavior in osteosarcoma in order to design targeted therapy for this disease. Previous reports have demonstrated that expression of VEGF/VEGFR1 in human osteosarcoma is associated with an aggressive clinical course (25, 26). Here we show that the highly metastatic K7M3 osteosarcoma cell line co-expresses VEGF/VEGFR1, thereby establishing an autocrine signaling mechanism associated with aggressive phenotypes, such as increased cell proliferation and decreased apoptosis *in vitro* and increased tumor growth and tumor-induced osteolysis *in vivo*. K7M3 cells express higher levels of VEGF/VEGFR1 than parental K12 cells and are insensitive to exogenous VEGF stimulation. That VEGF/VEGFR1 expression, VEGFR1 phosphorylation, cell viability, and cell proliferation are all significantly decreased by inhibition of VEGF/R1 signaling in K7M3 cells, but not K12 cells, suggests that the former cell line is stimulated by an autocrine VEGF/R1 signaling mechanism. Similar findings were observed in aggressive human osteosarcoma 143B cells and less aggressive, parental TE85 cells.

In addition, siRNA-mediated knockdown of VEGFR1 expression in K7M3 cells significantly reduced cell proliferation and induced apoptosis of K7M3 cells. K7M3 cells selected for high levels of VEGFR1 expression show increased proliferative capacity and VEGF production *in vitro* and *in vivo*. Finally, we show heterogeneity of VEGF/VEGFR1 co-expression in human osteosarcoma samples, which corresponds to the variation in VEGFR1 expression seen in the K7M3 cell line by flow cytometry.

VEGF secretion by malignant cells drives autocrine stimulation of VEGFR1 signaling and tumor cell proliferation (16, 27). Interestingly, autocrine VEGF/R1 signaling has been described only in highly metastatic or particularly aggressive cancer cell lines. Similar to our findings with K7M3 osteosarcoma cells, other investigators have reported different efficiencies of tumor growth in melanoma cell lines sorted for different levels of VEGFR1 expression (28).

Consistent with our *in vitro* data, we found that tumors produced by osteosarcoma cells selected for increased VEGFR1 expression grew faster and caused more bone destruction than tumors derived from osteosarcoma cells with low levels of VEGFR1 expression. In addition to autocrine mitogenic signals, another possible explanation for the more aggressive behavior seen in VEGFR1-high osteosarcoma cells is increased angiogenesis, as VEGFR1 signaling stimulates increased VEGF secretion by these cells and results in a vigorous angiogenic response *in vivo*. Therefore, although increased VEGF expression may directly induce proliferation of only a small subset of cells, it may indirectly stimulate proliferation in nearby tumor cells by increased local angiogenesis. Supporting this concept, immunofluorescence for Ki67 showed a higher proliferative index in VEGF/R1-positive regions of osteosarcoma *in vivo*.

Although somewhat controversial, increased VEGF expression has been associated with poor outcomes in patients with osteosarcoma (4, 29). Here we also show that chemotherapy-naïve human osteosarcoma cells variably coexpress VEGF/VEGFR1. The spatial heterogeneity of VEGF/VEGFR1 expression in osteosarcoma may account for the discrepancies about the prognostic significance of this marker. Future studies of a well-annotated clinical cohort are necessary to determine the prognostic significance of VEGF/R1 coexpression in osteosarcoma. The data presented here support the hypothesis that coexpression VEGF and VEGFR1 identifies a subpopulation of osteosarcoma cells with intrinsically higher potential for aggressive clinical behavior.

A limitation of the experimental model used in this study is that pulmonary metastasis does not become detectable until around 6 weeks after tumor cell inoculation. As the primary tumor grows rapidly and the mice become lame, they must be euthanized (or have the affected limb amputated) 3 to 4 weeks after tumor cell inoculation (23). Therefore, distant metastasis is not evaluable in this model and other methodologies are necessary to address the role of VEGF/R1 signaling in osteosarcoma metastasis.

Inhibition of VEGF effectively suppresses osteosarcoma angiogenesis in a murine model of osteosarcoma (9). Because blockade of autocrine VEGF/R1 signaling also inhibits proliferation and survival of an aggressive subpopulation of tumor cells *in vitro*, VEGF/R1 signaling may be highly relevant targetable pathway in osteosarcoma. Whether colocalization of VEGF-A/VEGFR1 within a threshold population of osteosarcoma cells correlates with prognosis is unknown, and future studies on a large and well-annotated clinical cohort will be necessary to address this question.

Disclosure of Potential Conflicts of Interest

H.S. Schwartz is a consultant/advisory board member of The Musculoskeletal Transplant Foundation. No potential conflicts of interest were disclosed by the other authors.

Authors' Contributions

Conception and design: T. Ohba, T. Ando, H.S. Schwartz, J.G. Schoenecker
Development of methodology: T. Ohba, J.G. Schoenecker
Acquisition of data (provided animals, acquired and managed patients, provided facilities, etc.): T. Ohba, H.A. Cole, J.G. Schoenecker
Analysis and interpretation of data (e.g., statistical analysis, biostatistics, computational analysis): T. Ohba, H. Haro, T. Ando, H.S. Schwartz, J.G. Schoenecker
Writing, review, and or revision of the manuscript: T. Ohba, J.M.M. Cates, H.A. Cole, D.A. Slosky, H. Haro, H.S. Schwartz, J.G. Schoenecker
Administrative, technical, or material support (i.e., reporting or organizing data, constructing databases): T. Ohba, H.A. Cole, H. Haro, J.G. Schoenecker
Study supervision: T. Ohba, T. Ando, H.S. Schwartz, J.G. Schoenecker

Acknowledgments

The authors thank Dr. J. Ichikawa for his development of the models used in this study and Dr. S. Borinstein for his critical review of this article.

Grant Support

This work was supported by the Caitlin Lovejoy Fund.

The costs of publication of this article were defrayed in part by the payment of page charges. This article must therefore be hereby marked *advertisement* in accordance with 18 U.S.C. Section 1734 solely to indicate this fact.

Received January 21, 2014; revised March 26, 2014; accepted April 9, 2014; published OnlineFirst April 23, 2014.

References

1. Ward WG, Mikaelian K, Dorey F, Mirra JM, Sassoon A, Holmes EC, et al. Pulmonary metastases of stage IIB extremity osteosarcoma and subsequent pulmonary metastases. J Clin Oncol 1994;12:1849–58.
2. Wunder JS, Nielsen TO, Maki RG, O'Sullivan B, Alman BA. Opportunities for improving the therapeutic ratio for patients with sarcoma. Lancet Oncol 2007;8:513–24.
3. Noh K, Kim KO, Patel NR, Staples JR, Minematsu H, Nair K, et al. Targeting inflammatory kinase as an adjuvant treatment for osteosarcomas. J Bone Joint Surg Am 2011;93:723–32.
4. Yu XW, Wu TY, Yi X, Ren WP, Zhou ZB, Sun YQ, et al. Prognostic significance of VEGF expression in osteosarcoma: a meta-analysis. Tumour Biol 2014;35:155–60.
5. Dvorak HF. Vascular permeability factor/vascular endothelial growth factor: a critical cytokine in tumor angiogenesis and a potential target for diagnosis and therapy. J Clin Oncol 2002;20: 4368–80.
6. Poon RT, Fan ST, Wong J. Clinical implications of circulating angiogenic factors in cancer patients. J Clin Oncol 2001;19:1207–25.
7. Savitskaya YA, Rico-Martinez G, Linares-Gonzalez LM, Delgado-Cedillo EA, Tellez-Gastelum R, Alfaro-Rodriguez AB, et al. Serum tumor markers in pediatric osteosarcoma: a summary review. Clin Sarcoma Res 2012;2:9.
8. Rastogi S, Kumar R, Sankineani SR, Marimuthu K, Rijal L, Prakash S, et al. Role of vascular endothelial growth factor as a tumour marker in osteosarcoma: a prospective study. Intl Orthop 2012;36: 2315–21.
9. Yin D, Jia T, Gong W, Yu H, Wooley PH, Mott MP, et al. VEGF blockade decelerates the growth of a murine experimental osteosarcoma. Int J Oncol 2008;33:253–9.
10. Sitohy B, Nagy JA, Dvorak HF. Anti-VEGF/VEGFR therapy for cancer: reassessing the target. Cancer Res 2012;72:1909–14.
11. Abdullah SE, Perez-Soler R. Mechanisms of resistance to vascular endothelial growth factor blockade. Cancer 2012;118:3455–67.
12. Mross K, Frost A, Steinbild S, Hedbom S, Buchert M, Fasol U, et al. A phase I dose-escalation study of regorafenib (BAY 73–4506), an inhibitor of oncogenic, angiogenic, and stromal kinases, in patients with advanced solid tumors. Clin Cancer Res 2012;18:2658–67.
13. Ferrara N, Gerber HP, LeCouter J. The biology of VEGF and its receptors. Nat Med 2003;9:669–76.
14. Hicklin DJ, Ellis LM. Role of the vascular endothelial growth factor pathway in tumor growth and angiogenesis. J Clin Oncol 2005;23: 1011–27.
15. Vincent L, Jin DK, Karajannis MA, Shido K, Hooper AT, Rashbaum WK, et al. Fetal stromal-dependent paracrine and intracrine vascular endothelial growth factor-a/vascular endothelial growth factor receptor-1 signaling promotes proliferation and motility of human primary myeloma cells. Cancer Res 2005;65:3185–92.
16. Lee TH, Seng S, Sekine M, Hinton C, Fu Y, Avraham HK, et al. Vascular endothelial growth factor mediates intracrine survival in human breast carcinoma cells through internally expressed VEGFR1/FLT1. PLoS Med 2007;4:e186.
17. Luu HH, Kang Q, Park JK, Si W, Luo Q, Jiang W, et al. An orthotopic model of human osteosarcoma growth and spontaneous pulmonary metastasis. Clin Exp Metastasis 2005;22:319–29.
18. Schmidt J, Strauss GP, Schon A, Luz A, Murray AB, Melchiori A, et al. Establishment and characterization of osteogenic cell lines from a spontaneous murine osteosarcoma. Differentiation 1988;39: 151–60.
19. Ning Y, Chen S, Li X, Ma Y, Zhao F, Yin L. Cholesterol, LDL, and 25-hydroxycholesterol regulate expression of the steroidogenic acute regulatory protein in microvascular endothelial cell line (bEnd.3). Biochem Biophys Res Commun 2006;342:1249–56.
20. Ichikawa J, Cole HA, Magnussen RA, Mignemi NA, Butler M, Holt GE, et al. Thrombin induces osteosarcoma growth, a function inhibited by low molecular weight heparin *in vitro* and *in vivo*: Procoagulant nature of osteosarcoma. Cancer 2012;118:2494–506.
21. Cole HA, Ichikawa J, Colvin DC, O'Rear L, Schoenecker JG. Quantifying intra-osseous growth of osteosarcoma in a murine model with radiographic analysis. J Orthop Res 2011;29:1957–62.
22. Nyangoga H, Mercier P, Libouban H, Basle MF, Chappard D. Three-dimensional characterization of the vascular bed in bone metastasis of the rat by microcomputed tomography (MicroCT). PLoS ONE 2011;6: e17336.
23. Khanna C, Prehn J, Yeung C, Caylor J, Tsokos M, Helman L. An orthotopic model of murine osteosarcoma with clonally related variants differing in pulmonary metastatic potential. Clin Exp Metastasis 2000;18:261–71.
24. Khanna C, Khan J, Nguyen P, Prehn J, Caylor J, Yeung C, et al. Metastasis-associated differences in gene expression in a murine model of osteosarcoma. Cancer Res 2001;61:3750–9.
25. Lee YH, Tokunaga T, Oshika Y, Suto R, Yanagisawa K, Tomisawa M, et al. Cell-retained isoforms of vascular endothelial growth factor (VEGF) are correlated with poor prognosis in osteosarcoma. Eur J Cancer 1999;35:1089–93.
26. Hassan SE, Bekarev M, Kim MY, Lin J, Piperdi S, Gorlick R, et al. Cell surface receptor expression patterns in osteosarcoma. Cancer 2012; 118:740–9.
27. Lichtenberger BM, Tan PK, Niederleithner H, Ferrara N, Petzelbauer P, Sibilia M. Autocrine VEGF signaling synergizes with EGFR in tumor cells to promote epithelial cancer development. Cell 2010; 140:268–79.
28. Frank NY, Schatton T, Kim S, Zhan Q, Wilson BJ, Ma J, et al. VEGFR-1 expressed by malignant melanoma-initiating cells is required for tumor growth. Cancer Res 2011;71:1474–85.
29. Kaya M, Wada T, Akatsuka T, Kawaguchi S, Nagoya S, Shindoh M, et al. Vascular endothelial growth factor expression in untreated osteosarcoma is predictive of pulmonary metastasis and poor prognosis. Clin Cancer Res 2000;6:572–7.